using the Agilent Bioanalyzer (Agilent Technologies, Palo Alto, CA, USA). Gene expression experiments were carried out using oligonucleotide-DNA microarrays. Detailed experimental procedures are described in Supplementary materials and methods.

Quantitative real-time PCR

cDNA was synthesized using First-Strand cDNA Synthesis kit (Amersham Biosciences, Piscataway, NJ, USA) as described in the manufacturer's protocol. The experimental procedures for real-time PCR are described in Supplementary materials and methods. The primer sequences are shown in Supplementary Table 1S.

Immunohistochemistry

Formalin-fixed paraffin sections (4 μm thick) were deparaffinized in xylene and rehydrated with graded ethanol. Endogenous peroxidase was inactivated by incubating the sections in 3% hydrogen peroxide for 30 min at room temperature. Antigen retrieval involved heat treatment for CDCP1 staining. Subsequently, the sections were incubated overnight at 4°C with polyclonal goat antibody against CDCP1 (Abcam, Cambridge, UK; 100:1 dilution), which was used in the previous study (Ikeda et al. 2006). After the primary antibody was washed, the sections were stained with Dako LSAB$^+$ system (Dako, Glostrup, Denmark) and counterstained with Meyer's hematoxylin. Biotin Blocking System (Dako) was used to examine CDCP1 expression in the normal kidney. The primary antibody was not used in the staining procedure for the control experiments and no specific staining was confirmed. CDCP1 staining was scored as follows: negative, <10% carcinoma cells stained and positive, ≥10% carcinoma cells stained. The percentage of stained cells was estimated in several fields (200×). Immunohistochemical scoring was performed in a single laboratory and was interpreted without any knowledge of the clinical data.

Statistics

Disease-specific survival was defined as the interval between surgery and death from RCC. Recurrence-free survival was defined as the interval between surgery and the subsequent appearance of local recurrence or metastatic disease.

To identify candidate genes whose expression levels correlated with disease-specific survival, the Cox proportional hazard model was fitted for each gene in the microarray experiment, as described previously (Neben et al. 2004). The cut-off level was defined as a hazard ratio (HR) of >2.5 and $P < 0.01$ in order to identify a set of genes associated with unfavorable survival.

The relationship between CDCP1 staining and clinical/pathological parameters was evaluated using Fisher's exact test in an immunohistochemical study. Survival curves were generated by the Kaplan–Meier method. The log-rank test was used to compare the survival curves and for univariate analysis. Multivariate analysis was conducted using the Cox proportional hazards model with a forward stepwise selection procedure. Statistical significance was set at $P < 0.05$. Statistical analyses were performed using the software package R (Ihaka and Gentlaman 1996) or Dr. SPSS II (SPSS, Chicago, IL, USA).

Results

Identification of candidate genes related to RCC survival by using microarray and quantitative real-time PCR

By analyzing the expression profile of 39 RCC samples, we identified 14 genes whose expression levels predicted unfavorable disease-specific survival (HR > 2.5, $P < 0.01$; Supplementary Table 2S). Of the 14 genes, we selected 9 genes, which are known to be involved in cell proliferation, apoptosis, or cancer development, and evaluated their expression in 65 samples by quantitative real-time PCR. According to the expression levels of the target gene, 65 patients were divided into two groups, and the disease-specific survival rate was compared (Supplementary Fig. 1S). Of the 9 genes analyzed, only CDCP1 was significantly associated with prognosis ($P = 0.039$). Thus, we performed immunohistochemical analysis on CDCP1 in the 230 patients, which was described as follows.

Immunohistochemical analysis of CDCP1

The patterns of CDCP1 expression in the carcinoma cells were observed as membranous and/or cytoplasmic staining (Fig. 1). The heterogeneous distribution of CDCP1 in both plasma membrane and cytoplasm has also been observed in colon cancers (Scherl-Mostageer et al. 2001). In the present study, CDCP1 staining was not detected in the glomerular and tubular cells of normal kidney. CDCP1 staining was positive in 77 cases (33.5%) and was significantly associated with the T stage, the presence of metastasis and the histological grade ($P = 0.028$, $P = 0.002$, and $P < 0.001$, respectively; Table 2).

Disease-specific survival

Univariate analysis of potential prognostic impact of clinical, pathological, and immunohistochemical parameters identified the presence of symptoms, T stage >2, the presence of nodal or distant metastasis, histological grade ≥3,

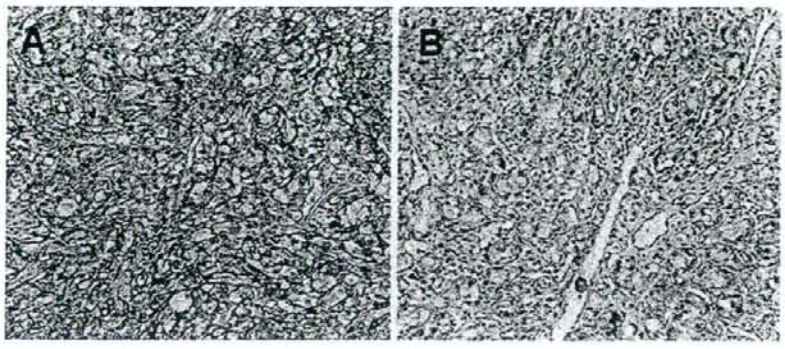

Fig. 1 Membranous (a) or cytoplasmic (b) staining of CDCP1 in the carcinoma cells

Table 2 Relationship between CDCP1 staining and clinicopathological factors

	CDCP1 staining		*P* value
	Negative	Positive	
Age (years)			
<60	58	30	0.887
60 or older	95	47	
Gender			
Male	108	61	0.205
Female	45	16	
Stage			
T1&T2	127	54	0.028
>T2	26	23	
N0M0	138	57	0.002
>N0 or M1	15	70	
Grade			
G1&G2	130	49	<0.001
G3&G4	23	28	

and CDCP1 positive staining as being significantly associated with shorter disease-specific survival ($P < 0.0001$, $P < 0.0001$, $P < 0.0001$, $P < 0.0001$, and $P = 0.0003$, respectively; Table 3). Disease-specific survival rates at 5 years for patients with CDCP1 positive and negative tumors were 71.7, and 90.8%, respectively (Fig. 2a). In the multivariate analysis including clinical/histological factors and the status of CDCP1 staining, the presence of metastasis and CDCP1 positive staining were significant predictors of shorter disease-specific survival ($P < 0.001$, $P = 0.042$, respectively; Table 3).

Recurrence-free survival

Recurrence-free survival was analyzed in 195 patients with localized RCC. Univariate analysis identified the presence of symptoms, T stage > 2, and CDCP1 positive staining as being significantly associated with shorter disease-specific survival ($P = 0.023$, $P = 0.0063$, and $P = 0.0022$, respectively; Table 4). Recurrence-free survival rates at 5 years for patients with CDCP1 positive and negative tumors were 83.6, and 93.9%, respectively (Fig. 2b). In the multivariate analysis, T stage > 2 and CDCP1 positive staining were significant predictors of shorter recurrence-free survival in the multivariate analysis ($P = 0.042$ and $P = 0.015$, respectively; Table 4).

Discussion

RCC comprises a heterogeneous group of tumors and is classified into various subtypes according to not only the morphological features but also the commonly identified genetic abnormalities (Bodmer et al. 2002). Conventional RCC is the major subtype of RCC, accounting for up to 80% of kidney cancers, and it is characterized by chromosome 3p deletion and frequent mutation of the von Hippel-Lindau gene. In the present study, we performed microarray-based screening of prognostic markers for conventional RCC. To our knowledge, five groups have previously reported gene signatures that defined RCC outcome based on transcriptional gene expression profiling (Takahashi et al. 2001; Vasselli et al. 2003; Jones et al. 2005; Kosari et al. 2005; Sultmann et al. 2005). Strikingly, there is almost no overlap among each set of significant genes identified in these studies. This is probably due to the difference in the design, methods and case subjects of each study. Of these studies, that by Kosari et al. identified 34 candidate biomarkers in a microarray experiment, and by immunohistochemistry in an independent group of patients, they confirmed that one of the candidate biomarkers (survivin) is inversely associated with prognosis (Kosari et al. 2005).

We demonstrated that CDCP1 is a potential prognostic marker for conventional RCC. In 2001, Scherl-Mostageer et al. first identified CDCP1 as the novel gene that is overexpressed in lung and colon carcinomas by using

Table 3 Univariate and mutivariate analyses of factors related to disease-specific survival

Variable	No. of patients ($n = 230$)	Univariate	Mutivariate		
		P value	Hazard ratio	95% CI	*P* value
Age (years)					
<60/60 or older	88/142	0.79	–	–	–
Gender					
Male/Female	169/61	0.48	–	–	–
Presentating symptoms					
Incidental/Symptomatic	144/86	<0.0001	–	–	–
Stage					
T1–2/>T2	181/49	<0.0001	–	–	–
N0M0/Other	195/35	<0.0001	34.92	14.58–83.63	<0.001
Grade					
G1–2/G3–4	179/51	<0.0001	–	–	–
CDCP1 expression					
Negative/Positive	153/77	0.0003	2.2	1.53–4.69	0.042

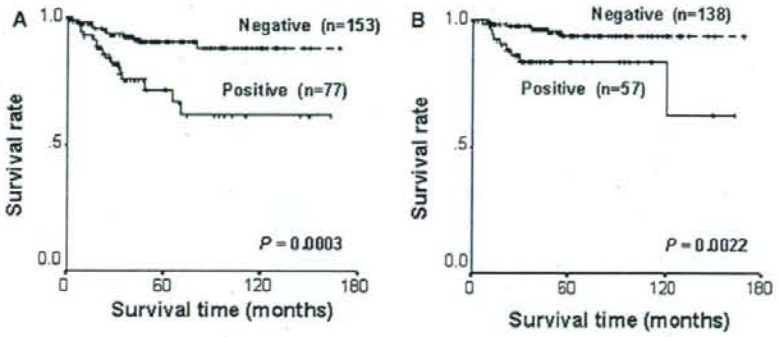

Fig. 2 Disease-specific (**a**) and recurrence-free (**b**) survivals according to CDCP1 staining

Table 4 Univariate and mutivariate analyses of factors related to recurrence-free survival

Variable	No. of patients ($n = 195$)	Univariate	Mutivariate		
		P value	Hazard ratio	95% CI	*P* value
Age (years)					
<60/60 or older	79/116	0.77	–	–	–
Gender					
Male/Female	139/56	0.72	–	–	–
Presentating symptoms					
Incidental/Symptomatic	139/56	0.023	–	–	–
Stage					
T1–2/>T2	165/30	0.0063	2.98	1.03–10.69	0.042
Grade					
G1–2/G3–4	166/29	0.23	–	–	–
CDCP1 expression					
Negative/Positive	138/57	0.0022	3.71	1.29–10.69	0.015

representational difference analysis and cDNA microarray (Scherl-Mostageer et al. 2001). Thereafter, Hooper et al. independently isolated CDCP1 as the protein that is preferentially expressed in metastatic variants of Hep3, an epidermoid carcinoma cell line, over non-metastatic variants (Hooper et al. 2003). CDCP1 is a transmembrane protein containing three extracellular CUB domains and intracellular tyrosine residues phosphorylated by the src

family. CUB domains are structurally related to immunoglobulins and are thought to play important roles in adhesion processes (Nentwich et al. 2002). CDCP1 reportedly interacts with other proteins involved in cell adhesion and cell-matrix association such as *N*-cadherin and matriptase (Bhatt et al. 2005), whose expression has been reported to correspond to RCC progression (Shimazui et al. 2006; Jin et al. 2006). In addition, the src family has been shown to not only form a complex with phosphorylated CDCP1 but also regulate the expression of CDCP1 protein in a cell cycle-dependent manner (Bhatt et al. 2005). Src is known to promote the motility and invasiveness of cancer cells (Yeatman 2004). Thus, CDCP1 might be implicated in cancer invasion and metastasis through src activation, although its precise function remains unclear. The activation of src has been reported in RCC cell lines (Yonezawa et al. 2005) but it has not been examined in primary tissues. Further analysis detailing the relationship between src activation and CDCP1 expression in RCC might become relevant to clinical practice because several src kinase inhibitors have been developed and have undergone clinical trials in other types of cancers (Yeatman 2004).

We recognize some limitations of the present study. First, among the nine candidate prognostic markers identified by using microarray experiment, only CDCP1 was linked to prognosis in qantitative real-time PCR assay. Thus, the quality control in microarray experiments may have been insufficient in the present study. Second, the population of immunohistochemical study was small and limited to patients referred to a single hospital. In addition, the median follow-up-time of 45.0 months for surviving patients was short. Thus, the present results need to be corroborated in independent patient populations. Recently, Kim et al. conducted a tissue array-based immunohistochemical study to investigate the prognostic value of several molecular markers including carbonic anhydrase 9, PTEN, and p53 (Kim et al. 2005). The combination of gene expression profiling and tissue-array technology might be a powerful approach for the identification of potential prognostic markers in RCC.

Acknowledgments This work was supported in part by NEDO (New Energy and Industrial Technology Development Organization) through its "Project for Developing Biotechnology IT Integration Equipment (P03013)."

References

Bhatt AS, Erdjument-Bromage H, Tempst P, Craik CS, Moasser MM (2005) Adhesion signaling by a novel mitotic substrate of src kinases. Oncogene 24:5333–5343

Bodmer D, van den Hurk W, van Groningen JJ, Eleveld MJ, Martens GJ, Weterman MA, van Kessel AG (2002) Understanding familial and non-familial renal cell cancer. Hum Mol Genet 11:2489–2498

Chuaqui RF, Bonner RF, Best CJ, Gillespie JW, Flaig MJ, Hewitt SM, Phillips JL, Krizman DB, Tangrea MA, Ahram M, Linehan WM, Knezevic V, Emmert-Buck MR (2002) Post-analysis follow-up and validation of microarray experiments. Nat Genet 32(Suppl):509–514

Gleave ME, Elhilali M, Fradet Y, Davis I, Venner P, Saad F, Klotz LH, Moore MJ, Paton V, Bajamonde A (1998) Interferon gamma-1b compared with placebo in metastatic renal-cell carcinoma. Canadian Urologic Oncology Group. N Engl J Med 338:1265–1271

Goldstein NS (1999) Grading of renal cell carcinoma. Urol Clin North Am 26:637–642

Hooper JD, Zijlstra A, Aimes RT, Liang H, Claassen GF, Tarin D, Testa JE, Quigley JP (2003) Subtractive immunization using highly metastatic human tumor cells identifies SIMA135/CDCP1, a 135 kDa cell surface phosphorylated glycoprotein antigen. Oncogene 22:1783–1794

Ihaka R, Gentlaman R (1996) R: a language for data analysis and graphics. J Comput Graph Stat 5:299–314

Ikeda JI, Morii E, Kimura H, Tomita Y, Takakuwa T, Hasegawa JI, Kim YK, Miyoshi Y, Noguchi S, Nishida T, Aozasa K (2006) Epigenetic regulation of the expression of the novel stem cell marker CDCP1 in cancer cells. J Pathol 210:75–84

Jin JS, Chen A, Hsieh DS, Yao CW, Cheng MF, Lin YF (2006) Expression of serine protease matriptase in renal cell carcinoma: correlation of tissue microarray immunohistochemical expression analysis results with clinicopathological parameters. Int J Surg Pathol 14:65–72

Jones J, Otu H, Spentzos D, Kolia S, Inan M, Beecken WD, Fellbaum C, Gu X, Joseph M, Pantuck AJ, Jonas D, Libermann TA (2005) Gene signatures of progression and metastasis in renal cell cancer. Clin Cancer Res 11:5730–5739

Kim HL, Seligson D, Liu X, Janzen N, Bui MH, Yu H, Shi T, Belldegrun AS, Horvath S, Figlin RA (2005) Using tumor markers to predict the survival of patients with metastatic renal cell carcinoma. J Urol 173:1496–1501

Kosari F, Parker AS, Kube DM, Lohse CM, Leibovich BC, Blute ML, Cheville JC, Vasmatzis G (2005) Clear cell renal cell carcinoma: gene expression analyses identify a potential signature for tumor aggressiveness. Clin Cancer Res 11:5128–5139

Lam JS, Shvarts O, Leppert JT, Figlin RA, Belldegrun AS (2005) Renal cell carcinoma 2005: new frontiers in staging, prognostication and targeted molecular therapy. J Urol 173:1853–1862

Maruyama R, Yamana K, Itoi T, Hara N, Bilim V, Nishiyama T, Takahashi K, Tomita Y (2006) Absence of Bcl-2 and Fas/CD95/APO-1 predicts the response to immunotherapy in metastatic renal cell carcinoma. Br J Cancer 95:1244–1249

Mejean A, Oudard S, Thiounn N (2003) Prognostic factors of renal cell carcinoma. J Urol 169:821–827

Motzer RJ, Russo P (2000) Systemic therapy for renal cell carcinoma. J Urol 163:408–417

Neben K, Korshunov A, Benner A, Wrobel G, Hahn M, Kokocinski F, Golanov A, Joos S, Lichter P (2004) Microarray-based screening for molecular markers in medulloblastoma revealed STK15 as independent predictor for survival. Cancer Res 64:3103–3111

Nentwich HA, Mustafa Z, Rugg MS, Marsden BD, Cordell MR, Mahoney DJ, Jenkins SC, Dowling B, Fries E, Milner CM, Loughlin J, Day AJ (2002) A novel allelic variant of the human TSG-6 gene encoding an amino acid difference in the CUB module. Chromosomal localization, frequency analysis, modeling, and expression. J Biol Chem 277:15354–15362

Scherl-Mostageer M, Sommergruber W, Abseher R, Hauptmann R, Ambros P, Schweifer N (2001) Identification of a novel gene, CDCP1, overexpressed in human colorectal cancer. Oncogene 20:4402–4408

Shimazui T, Oosterwijk E, Debruyne FM, Schalken JA (1996) Molecular prognostic factor in renal cell carcinoma. Semin Urol Oncol 14:250–255

Shimazui T, Kojima T, Onozawa M, Suzuki M, Asano T, Akaza H (2006) Expression profile of *N*-cadherin differs from other classical cadherins as a prognostic marker in renal cell carcinoma. Oncol Rep 15:1181–1184

Stadler WM (2005) Targeted agents for the treatment of advanced renal cell carcinoma. Cancer 104:2323–2333

Sultmann H, von Heydebreck A, Huber W, Kuner R, Buness A, Vogt M, Gunawan B, Vingron M, Fuzesi L, Poustka A (2005) Gene expression in kidney cancer is associated with cytogenetic abnormalities, metastasis formation, and patient survival. Clin Cancer Res 11:646–655

Takahashi M, Rhodes DR, Furge KA, Kanayama H, Kagawa S, Haab BB, Teh BT (2001) Gene expression profiling of clear cell renal cell carcinoma: gene identification and prognostic classification. Proc Natl Acad Sci USA 98:9754–9759

Vasselli JR, Shih JH, Iyengar SR, Maranchie J, Riss J, Worrell R, Torres-Cabala C, Tabios R, Mariotti A, Stearman R, Merino M, Walther MM, Simon R, Klausner RD, Linehan WM (2003) Predicting survival in patients with metastatic kidney cancer by gene-expression profiling in the primary tumor. Proc Natl Acad Sci USA 100:6958–6963

Yeatman TJ (2004) A renaissance for SRC. Nat Rev Cancer 4:470–480

Yonezawa Y, Nagashima Y, Sato H, Virgona N, Fukumoto K, Shirai S, Hagiwara H, Seki T, Ariga T, Senba H, Suzuki K, Asano R, Hagiwara K, Yano T (2005) Contribution of the Src family of kinases to the appearance of malignant phenotypes in renal cancer cells. Mol Carcinog 43:188–197

J Pharmacol Sci 107, 1 – 7 (2008)

Journal of Pharmacological Sciences

Forum Minireview

Pharmacogenomics of Cardiovascular Pharmacology: Development of an Informatics System for Analysis of DNA Microarray Data With a Focus on Lipid Metabolism

Yoshiyuki Takahara[1,*], Tomoko Kobayashi[1], Kazuhisa Takemoto[1], Tetsuya Adachi[2], Ken Osaki[3], Kozo Kawahara[3], and Gozoh Tsujimoto[2]

[1]*PharmaFrontier Co., Ltd., 448-5 Kajii-cho, Kamigyo-ku, Kyoto 602-0841, Japan*
[2]*Department of Genomic Drug Discovery Science, Graduate School of Pharmaceutical Sciences, Kyoto University, 46-29 Yoshida Shimoadachi-cho, Sakyo-ku, Kyoto 606-8501, Japan*
[3]*World Fusion Co., Ltd., 2-15-15, Nihonbashi Ningyo-cho, Chuo-ku, Tokyo 103-0013, Japan*

Received February 15, 2008; Accepted March 14, 2008

Abstract. Genome-wide gene-expression data from DNA-microarray technology and molecular-network data from computational text-mining have led to a paradigm shift in biological research. However, interpretation of the huge amount of data is a bottleneck. We have developed an informatics system, which we refer to as bioSpace Explorer, that can extract pathways and molecules of interest from genome-wide data and show the mutual relationships among these pathways and molecules. Differentiation of 3T3-L1 cells into adipocytes and the action of a peroxisome proliferator-activated receptor gamma (PPARγ) agonist or α-linolenic acid on this process was analyzed with bioSpace Explorer. The results suggested a biological basis for adipocyte differentiation and a strategy to enhance lipid oxidation in adipocytes. Clustered changes of molecules were apparent in the insulin, Wnt, and PPARγ signaling pathways and in the lipogenesis, lipid oxidation, and lipid transport pathways during cell differentiation. A PPARγ agonist enhanced lipid oxidation in adipocytes and α-linolenic acid gave similar results to the PPARγ agonist. An analysis of sex hormone and thyroid hormone, in addition to PPARγ signaling, suggested that these molecules are important for enhancement of lipid oxidation in adipocytes. The results indicate the utility of bioSpace Explorer for biological research on genome-wide molecular networks.

Keywords: DNA microarray, adipocyte, lipid oxidation, peroxisome proliferator-activated receptor gamma (PPARγ), text-mining, pharmacogenomics, network analysis

1. Genome-wide molecular network database and DNA microarray data

Sequencing of the human genome has been accompanied by publication of a large amount of information on the interactions of products of these genes. This information can be used to construct molecular networks using computational text-mining (1). On the other hand, DNA microarrays provide genome-wide information on gene expression and provide information on dynamic expression behavior of a genome-wide molecular network. This genome-wide view has produced a paradigm shift in biological research, but it is difficult to interpret the biological significance of the huge amount of available data. Therefore, we have developed an informatics system, which we refer to as bioSpace Explorer, which includes software and a database that permit easier understanding of the biological meaning of DNA-microarray data. Initially, we developed bioSpace Explorer specifically for analysis of lipid metabolism. We chose to develop the informatics tool for a given research field because an overall tool for all fields may

*Corresponding author. ytakahara@pharmafrontier.co.jp
Published online in J-STAGE
doi: 10.1254/jphs.08R02FM

be too complex for data handling and insufficiently sensitive for each field.

bioSpace Explorer has three layers of networks. The first layer, the 'Entrance-View', shows a comprehensive overview (which we call the bird's eye view) of lipid metabolism and other networks that regulate lipid metabolism. In the 'Entrance-View', the number of molecules is limited to around 300; this permits a comprehensive understanding of changes in gene expression and allows selection of networks of interest. The second layer includes 33 fundamental pathways that are well-known in textbooks or public databases. Detailed molecular information, such as the presence of isozymes, is listed in these networks, allowing the details of each network to be examined, with the potential to focus in on networks and molecules of interest.

The chosen networks or molecules can be linked with related molecules using the 'Expand Pathway' option in the third layer, which displays unique networks that are prepared for a given study. A genome-wide molecular network database and the Expand Pathway system are provided by Ariadne Genomics, Inc. (Rockville, MD, USA) (2), and bioSpace Explorer serves as an interface between the Expand Pathway system and a particular study. Expand Pathway is designed to expand the search for related molecules from molecules of interest; for example, related molecules that are directly linked to a selected molecule (direct relationship) or are linked through a third molecule (one-neighbor relationship) can be shown with Expand Pathway. Genes can also be linked to each other to make functional clusters using this system. These two methods are usually used in the third layer of bioSpace Explorer. In the current paper, we verified the use of bioSpace Explorer for analysis of lipid metabolism.

2. Changes in lipid metabolism during adipocyte differentiation and effects of a PPARγ agonist and a long-chain unsaturated fatty acid on these changes

The 3T3-L1 cell line has been established as a model of adipocyte differentiation, and DNA-microarray analysis of 3T3-L1 cells has been widely reported (3) with examination of events from the early to middle stages of differentiation of these cells. Differentiated adipocytes produce harmful adipocytokines in the late phase (from day 14 to day 21 in 3T3-L1 cells). Obese people have many adipocytes that are related to the onset of metabolic syndrome (4). We examined lipid metabolism in the late phase and tried to find a treatment for enhancement of fatty acid beta-oxidation to consume lipids stored in adipocytes.

Fourteen days after induction of 3T3-L1 differentiation to adipocytes, 10 μM Troglitazone (Tro), a peroxisome proliferator-activated receptor gamma (PPARγ) agonist, or 100 μM α-linolenic acid were added for 7 days (control cells were also incubated without addition of Tro or α-linolenic acid). DNA microarray data were determined at five time-points: P1 (2 days before induction), P2 (14 days after induction), P3 (21 days after induction), P4 (21 days after induction with α-linolenic acid), and P5 (21 days after induction with Tro) using GeneChip (Mouse Genome 430 2.0 Array; Affymetrix Inc., Sunnyvale, CA, USA). The results were input into bioSpace Explorer for analysis of lipid metabolism.

3. 'Entrance View' and 'Fundamental Pathways'

Analysis in 'Entrance View' of changes in gene expression between the P2/P1, P3/P2, and P5/P3 time points showed clustered changes of molecules in the insulin, Wnt, and PPARγ signaling pathways and in lipogenesis, lipid oxidation, and lipid transport, as shown in Table 1. An example of the Entrance View screen for the P3/P2 comparison is shown in Fig. 1. After induction in the early phase of adipocyte formation, genes in the insulin signaling, Wnt signaling, lipogenesis, and lipid oxidation pathways were down-regulated, but key molecules for differentiation, such as PPARγ and molecules for lipid transfer, were up-regulated.

Table 1. Changes in functionally clustered genes during adipocyte differentiation

Pathways	P2 (day 14) / P1 (day 2)	P3 (day 21) / P2 (day 14)	P5 (Tro, day 21) / P3 (day 21)
Insulin signaling	↓	↑	↓
Wnt signaling	↓	↑	↓
Lipogenesis	↓	↑	↑
Lipid oxidation	↓	↑	↑
Lipid transport	↑	↑	↑
PPARγ signaling	↑	↑	↑

↑ Clustered up-regulation of gene expression. ↓ Clustered down-regulation of gene expression.

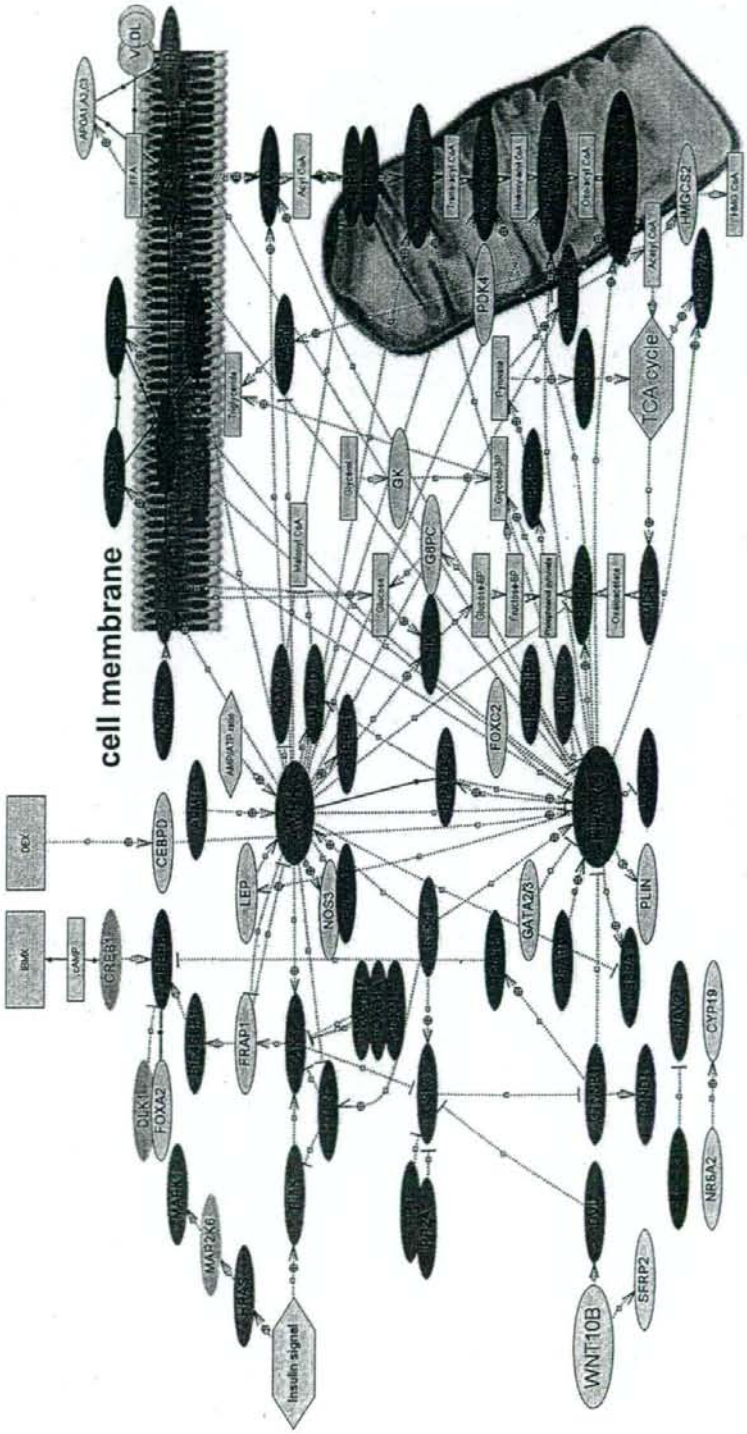

Fig. 1. An example of the 'Entrance View' layer. Ratio of expression levels of genes at the P3/P2 time points. Up-regulation over 1.5 is indicated in red and down-regulation lower than 0.67 is indicated in green. The color depth is proportional to the value of the ratio.

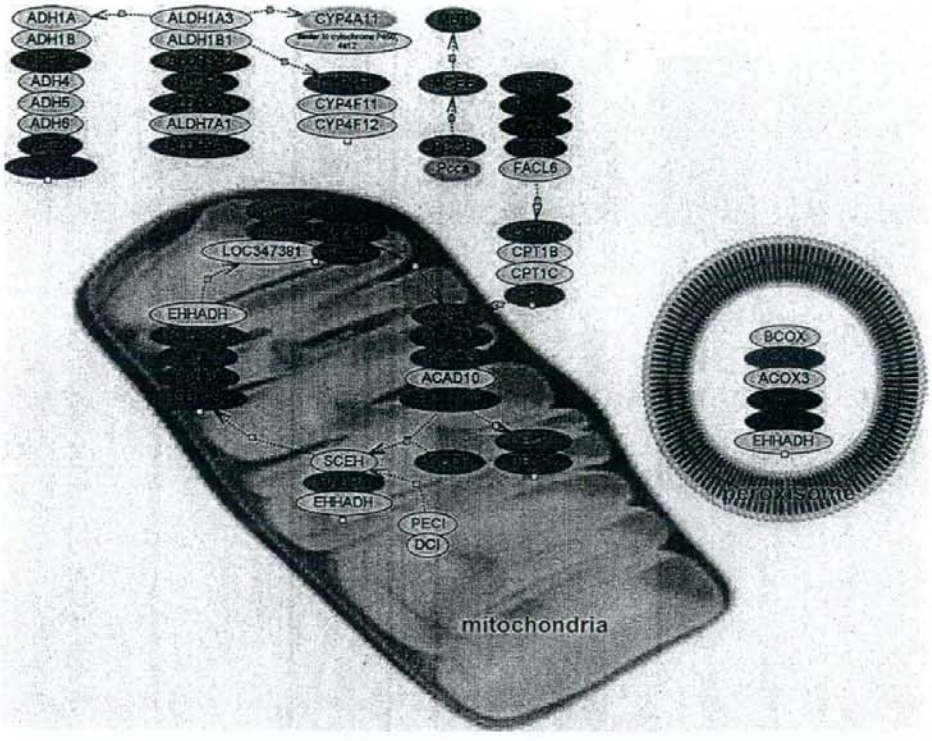

Fig. 2. An example of the 'Fundamental Pathway' layer. The lipolysis pathway including beta-oxidation is shown. Ratio of the expression levels of genes at the P3/P2 time points. Up-regulation over 1.5 is indicated in red and down-regulation lower than 0.67 is indicated as green. The color depth is proportional to the value of the ratio.

Alteration of expression of pathway members can be checked in detail in the 'Fundamental Pathway' display, as shown in Fig. 2. Adipocytes serve as storage tanks for lipid, based on typical characteristics of white adipocytes. Genes associated with insulin signaling, Wnt signaling, lipogenesis, and lipid oxidation were up-regulated in the late phase of differentiation. In the presence of Tro, genes associated with lipogenesis, lipolysis, and beta-oxidation were up-regulated, but those associated with insulin and Wnt signaling were down-regulated. Treatment with α-linolenic acid did not induce any changes of clustered molecules in the pathways shown in 'Entrance View'.

4. Identification of molecules that enhance β-oxidation in the late phase of adipocyte differentiation using 'Expand Pathway'

PPARγ is a key molecule in adipocyte differentiation (5) and expression of PPARγ increased from the early phase to the late phase, before reaching a plateau in the late phase. Fatty acid beta-oxidation is suppressed in the early phase despite PPARγ expression, which may be due to expression of regulatory molecules linked to PPARγ that are required for activation of the fatty acid beta-oxidation pathway. Candidate genes that enhance fatty acid beta-oxidation should change in expression in the late phase and the expression change should not be reversed in the presence of a PPARγ agonist. Transcription factors showing this behavior were selected from the microarray data and used in the 'Expand Pathway' system to identify molecules with a direct or one-neighbor link to PPARγ; 155 genes were selected using this process and classified based on function, as follows: 1) nuclear factors and their co-factors, 2) circadian rhythm, 3) lipid metabolism, 4) cell cycle and apoptosis, 5) general transcription factors, and 6) other molecules required for signal transduction. Eighty molecules were chosen from functional categories 1), 2), and 3) and published relationships between the selected molecules

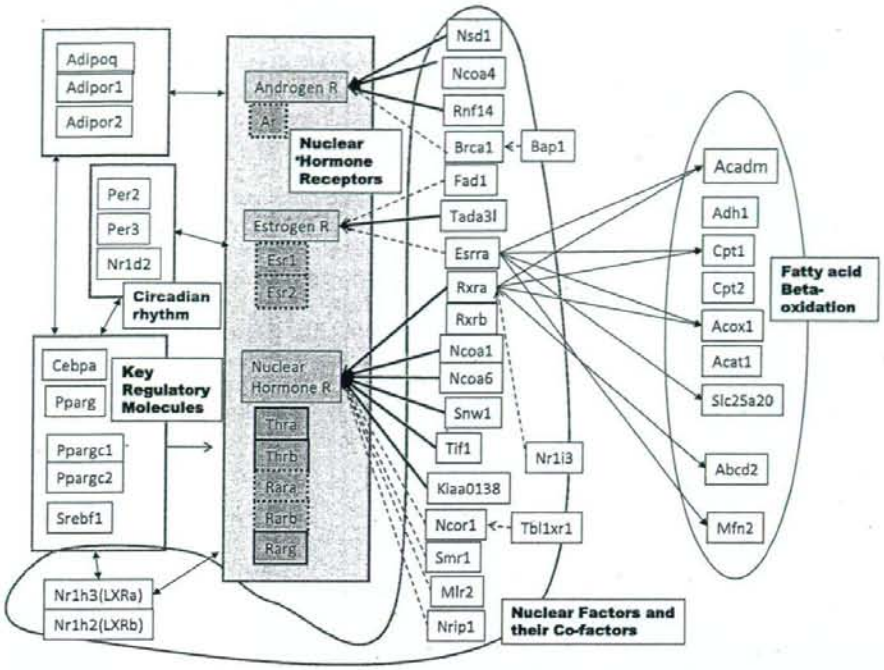

Fig. 3. Nuclear factors and transcription factors related to fatty acid beta-oxidation that were up-regulated in the late phase of adipocyte differentiation. Genes related to nuclear hormone receptors, such as estrogen receptors, androgen receptors, thyroid hormone receptors, and/or retinoid receptors, were identified. Genes up-regulated in the late phase of adipocyte differentiation are colored white. Genes for which expression did not change in the late phase of adipocyte differentiation are colored gray. Genes expressed at an intensity of less than 10 are outlined with a broken line. All white-colored genes have a relationship with the beta-oxidation pathway. Thick and broken lines indicate direct enhancement and inhibition of gene expression, respectively, by a particular gene.

and beta-oxidation were investigated, leading to a final selection of 23 molecules.

Nuclear hormone receptors such as androgen receptors, estrogen receptors, thyroid hormone receptors, and retinoid receptors were common among the selected molecules, as shown in Fig. 3. Since the culture medium for 3T3L1 cells contained thyroid hormone, differentiated adipocytes become responsive to thyroid hormone in the late phase and change their lipid metabolism status. An effect of thyroid hormone on energy metabolism in adipocytes has been reported (6) and our results provide an understanding of the molecular basis of this effect. Additionally, the balance of sex hormones is likely to be important for lipid metabolism of well-differentiated adipocytes under physiological conditions. PPARGC1/2 and ESRRA/B were up-regulated in the late phase and are related to beta-oxidation, which seems to be another important pathway associated with the selected molecules (data not shown). These molecules have been reported to dimerize to promote expression of important genes in the beta-oxidation pathway, such as ACOX1 and ACADAM (7). Up-regulation of PPARGC in the late phase may have a major effect on lipid metabolism, including beta-oxidation, because PPARGC has a role as a co-factor for many nuclear factors.

5. Analysis of the influence of α-linolenic acid on adipocytes

Half of the genes up-regulated by α-linolenic acid were identical to those up-regulated by the PPARγ agonist Tro. Similarly, genes down-regulated with α-linolenic acid were also down-regulated with Tro, as shown in Table 2. This suggests that most genes for which expression is altered by α-linolenic acid are regulated through the PPARγ pathway. Relationships between genes showing altered expression and members

Table 2. Comparison of changes in gene expression between treatment with α-linolenic acid and troglitazone, a PPARγ agonist

+ α-Linolenic acid	+ Troglitazone	
Up-regulated	up-regulated	54.7%
	no change	33.3%
	down-regulated	12.0%
Down-regulated	up-regulated	4.6%
	no change	50.6%
	down-regulated	44.8%

Half of the genes that changed in expression with α-linolenic acid showed similar changes with troglitazone.

of the beta-oxidation pathway were investigated using the 'Expand Pathway' system. Using direct and one-neighbor relationships in 'Expand Pathway', molecules related to members of the beta-oxidation pathway were selected from genes up-regulated by α-linolenic acid. Twenty genes were selected and divided into five functional categories: enhancement of energy expenditure as heat, nuclear factor/nuclear hormone receptors and their co-factors, lipolysis, lipid transport, and adipocyte differentiation, as shown in Fig. 4. Most of these genes were also up-regulated by the PPARγ agonist, suggesting that the mechanism of enhancement of beta-oxidation by α-linolenic acid occurs via PPARγ. However several genes that were up-regulated with α-linolenic acid were down-regulated or did not change in expression with the PPARγ agonist, which suggests the presence of a second pathway independent of PPARγ. For example, the signaling through a membrane receptor, GPR120, has been reported to respond to α-linolenic acid (8), and this speculative suggestion was generated using DNA-microarray data in bioSpace Explorer. Although the findings require experimental validation, they serve as an example of how bioSpace Explorer can contribute to biological research by providing a new perspective on genome-wide molecular networks.

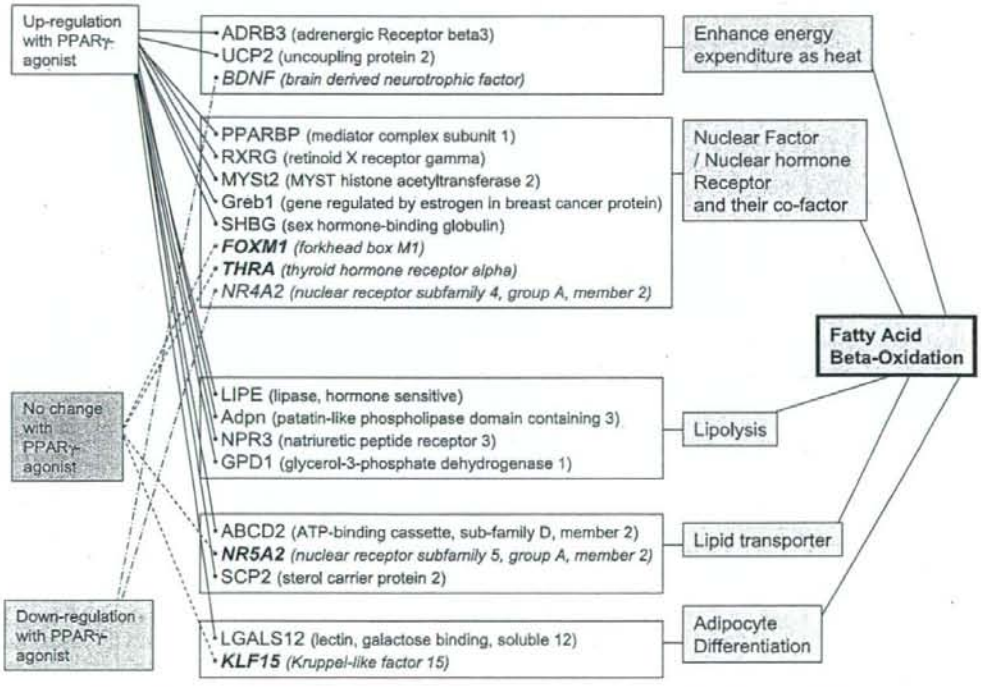

Fig. 4. Functionally categorized genes that were up-regulated in the presence of α-linolenic acid and were related to fatty acid beta-oxidation. Most genes that were up-regulated in the presence of α-linolenic acid and were related to fatty acid beta-oxidation showed similar changes with troglitazone, a PPARγ-agonist. However, some genes that were up-regulated by α-linolenic acid did not change or were down-regulated with troglitazone.

References

1 Krallinger M, Erhardt RA, Valencia A. Text-mining approaches in molecular biology and biomedicine. Drug Discovery Today. 2005;10:439–445.

2 Sivachenko AY, Yuryev A. Pathway analysis software as a tool for drug target selection, prioritization and validation of drug mechanism. Expert Opin Ther Targets. 2007;11:411–421.

3 Soukas A, Socci ND, Saatkamp BD, Novelli S, Fiedman JM. Direct transcriptional profiles of adipogenesis in vivo and in vitro. J Biol Chem. 2001;276:34167–34174.

4 Matsuzawa Y. Adipocytokines and metabolic syndrome. Semi Vasc Med. 2005;5:34–39.

5 Sharma AM, Staels B. Peroxisome proliferator-activated receptor gamma and adipose tissue – understanding obesity-related changes in regulation of lipid and glucose metabolism. J Clin Endocrinol Metab. 2007;92:386–395.

6 Mariash CN. Thyroid hormone and the adipocyte. J Clin Endcrinol Metab. 2003;88:5603–5604.

7 Kamei Y, Ohizumi H, Fujitani Y, Nemoto T, Tanaka T, Kakizuka A, et al. PPARgamma coactivator 1beta/ERR ligand 1 is an ERR protein ligand, whose expression induces a high-energy expenditure and antagonizes obesity. Proc Natl Acad Sci U S A. 2003;100:12378–12383.

8 Hirasawa A, Tsumaya K, Awaji T, Katsuma S, Adachi T, Yamada M, et al. Fatty acids regulate gut incretin glucagon-like peptide-1 secretion through GPR120. Nat Med. 2005;11: 90–94.

Secreted CXCL1 Is a Potential Mediator and Marker of the Tumor Invasion of Bladder Cancer

Hiroaki Kawanishi,[1] Yoshiyuki Matsui,[1] Masaaki Ito,[1] Jun Watanabe,[1] Takeshi Takahashi,[1] Koji Nishizawa,[1] Hiroyuki Nishiyama,[1] Toshiyuki Kamoto,[1] Yoshiki Mikami,[2] Yoshinori Tanaka,[4] Giman Jung,[4] Hideo Akiyama,[4] Hitoshi Nobumasa,[4] Parry Guilford,[5,6] Anthony Reeve,[5] Yasushi Okuno,[3] Gozoh Tsujimoto,[3] Eijiro Nakamura,[1] and Osamu Ogawa[1]

Abstract

Purpose: The purpose of this study was to identify proteins that are potentially involved in the tumor invasion of bladder cancer.

Experimental Design: We searched for the candidate proteins by comparing the profiles of secreted proteins among the poorly invasive human bladder carcinoma cell line RT112 and the highly invasive cell line T24. The proteins isolated from cell culture supernatants were identified by shotgun proteomics. We found that CXCL1 is related to the tumor invasion of bladder cancer cells. We also evaluated whether the amount of the chemokine CXCL1 in the urine would be a potential marker for predicting the existence of invasive bladder tumors.

Results: Higher amount of CXCL1 was secreted from highly invasive bladder carcinoma cell lines and this chemokine modulated the invasive ability of those cells *in vitro*. It was revealed that CXCL1 regulated the expression of matrix metalloproteinase-13 *in vitro* and higher expression of CXCL1 was associated with higher pathologic stages in bladder cancer *in vivo*. We also showed that urinary CXCL1 levels were significantly higher in patients with invasive bladder cancer (pT1-4) than those with noninvasive pTa tumors ($P = 0.0028$) and normal control ($P < 0.0001$). Finally, it was shown that CXCL1 was an independent factor for predicting the bladder cancer with invasive phenotype.

Conclusions: Our results suggest that CXCL1 modulates the invasive abilities of bladder cancer cells and this chemokine may be a potential candidate of urinary biomarker for invasive bladder cancer and a possible therapeutic target for preventing tumor invasion.

Bladder cancer is the fourth most common cancer in the United States and it will be responsible for the death of an estimated 13,060 persons in the United States alone during 2006 (1, 2). Bladder cancer is generally classified into superficial (non-muscle invasive) or muscle-invasive cancer based on the natural history of these tumors. Most bladder cancers (~80%) present as superficial tumors, which include Ta (noninvasive) or T1 (lamina propria invasive) tumor. Among these superficial tumors, ~70% recur after transurethral resection and 10% to 20% show progression to become muscle-invasive (T2-4) tumors. T1 tumors are more likely to progress to muscle-invasive disease (25-40%) than Ta tumors (3-4%; ref. 3). Muscle-invasive cancer has a much less favorable prognosis than superficial cancer (4). Due to the unfavorable prognosis of muscle-invasive cancer, there is considerable interest in developing markers that can identify superficial cancers with a high risk of progression. The identification of this type of marker will contribute to the early detection of life-threatening invasive bladder cancer and the improvement of the prognosis of this disease.

Multifocality and frequent recurrence is also another characteristic of bladder cancers (5). Multifocal tumors often present with varying degrees of stage and grade. Most studies have found only monoclonal tumors. The presence of shared genetic changes in all tumors resected from individual patients suggests that these are related lesions that have evolved from a single altered cell clone. However, there are some examples of more than one unrelated monoclonal tumor in the same bladder (oligoclonality), and this is not surprising given the association of transitional cell carcinoma risk with smoking and the pan-urothelial carcinogenic insult associated with this (6). There are two types of bladder cancer with fundamentally

Authors' Affiliations: Departments of [1]Urology and [2]Pathology, Graduate School of Medicine and [3]Department of Genomic Drug Discovery Science, Graduate School of Pharmaceutical Sciences, Kyoto University, Kyoto, Japan; [4]New Frontiers Research Laboratories, Toray Industries, Inc., Kanagawa, Japan; and [5]Cancer Genetics Laboratory, University of Otago; [6]Pacific Edge Biotechnology Ltd., Dunedin, New Zealand

Received 8/5/07; revised 12/29/07; accepted 1/17/08.

Grant support: Grant-in-Aid from the Ministry of Education, Culture, Sports, Science and Technology of Japan, Kurozumi Medical Foundation, and Takeda Science Foundation (E. Nakamura) and The New Energy and Industrial Technology Development Organization of Japan (O. Ogawa).

The costs of publication of this article were defrayed in part by the payment of page charges. This article must therefore be hereby marked *advertisement* in accordance with 18 U.S.C. Section 1734 solely to indicate this fact.

Note: Supplementary data for this article are available at Clinical Cancer Research Online (http://clincancerres.aacrjournals.org/).

Requests for reprints: Eijiro Nakamura, Department of Urology, Kyoto University Graduate School of Medicine, 54 Shogoinkawahara-cho, Sakyo-ku, 606-8507 Kyoto, Japan. Phone: 81-75-751-3325; Fax: 81-75-761-3441; E-mail: hap@kuhp.kyoto-u.ac.jp.

doi:10.1158/1078-0432.CCR-07-1922

different genetic alterations and clinical outcome. Whereas noninvasive tumors are genetically stable and characterized by frequent FGFR3 mutations and deletions of chromosome 9q, invasive bladder cancer are characterized by gross chromosomal instability and many genetic alterations. Alterations in both p53 and Rb tumor gene suppressor pathways are well documented in invasive bladder cancer. Additionally, numerous markers, such as cell adhesion molecules, tumor-associated antigens, proliferating antigens, and cell cycle regulatory proteins, have been identified, which correlate to some extent with tumor stage and prognosis (7). However, the power of many of these biomarkers in detecting superficial disease or predicting the clinical outcome of individual tumors is limited, and alternative markers are still in demand.

Secreted proteins determine, control, and coordinate many of the biological processes in organisms, such as cellular growth, differentiation, and tumorigenesis (8). After the completion of the Human Genome Project, many researchers have hypothesized that the best cancer biomarkers will probably be secreted proteins (9). Thus, great interest is currently being focused on the characterization of proteins secreted by isolated tumor cells and neoplastic tissues to identify novel biomarkers and new molecular targets for therapy.

Approximately 20% to 25% of all cellular proteins undergo secretion (10); however, the quantity of each protein secreted is usually very low. Analysis of culture supernatants after incubation of cells seems to be a reasonable way to identify such secreted proteins. However, even minor contamination with protein-rich FCS can easily mask secreted proteins of interest. Recently, we established a new method for analyzing the proteins in cell culture supernatants by using serum-free medium. Using this method, we identified clusterin as a marker for the hypoxia-inducible factor–independent function of von Hippel-Lindau protein and revealed its role in the development of familial pheochromocytoma (11, 12). In these studies, secreted proteins in the serum-free medium were precipitated with trichloroacetic acid and analyzed by two-dimensional PAGE. Then, protein spots of interest were identified by mass spectrometry (MS) analysis. Although two-dimensional PAGE provides information about the position of protein spots, it may not be so effective for detecting scarce secreted proteins (13). In the present study, we improved our method by using multidimensional shotgun proteomics, a powerful proteomics analysis tool with a high efficiency to identify hundreds of proteins in a single run (14, 15). Using this method, we compared the proteome of secreted proteins in the culture supernatant from bladder cancer cell lines with different invasive phenotypes and found that CXCL1 is overexpressed in invasive bladder cancer.

Materials and Methods

Cell lines and cell culture. Six human bladder cancer cell lines were used: DSH1 (16), KU-7 (17), RT112 (18), UMUC-3 (19), 5637 (20), and T24 (21). The cell lines were cultured in RPMI 1640 (Sigma Chemical Co.) supplemented with 10% FCS, 12.5 mmol/L HEPES, and penicillin-streptomycin at 37°C in 5% CO_2.

Cell invasion assay. BD Biocoat Matrigel Invasion Chambers (Becton Dickinson) were used. Cells were suspended to a concentration of 1×10^5/mL in serum-free RPMI 1640. The cell suspension (500 μL) was added to the insert of the Matrigel-coated invasion chamber (24 well and 8-μm pore size) and incubated with RPMI 1640 with 10% FCS in the bottom of the chamber at 37°C in 5% CO_2. Incubation time was modified according to the invasive ability of the cell lines. Noninvading cells were removed by wiping with cotton swabs and the cells that attached to the lower surface of the membrane were fixed with 70% ethanol. Cells were then stained with hematoxylin and counted using a microscope (Eclipse E1000M, Nikon). Invading cells were quantified by counting the number of cells in the five densest spots identified on the lower surface of the filter within a single ×200 field. Each experiment was done in triplicate.

Processing of cell culture supernatants. RT112 and T24 were grown to 70% to 80% confluence in RPMI 1640 with 10% FCS in 100-mm dishes. The cells were washed with PBS thrice and cultured in 10 mL serum-free RPMI 1640. In pilot experiments, we found that these cell lines proliferate for at least 2 d when grown in serum-free RPMI 1640 (data not shown). Twenty-four hours later, cell culture supernatants were collected from four dishes (40 mL) and centrifuged at 150,000 × *g* and 4°C for 30 min in a Beckman Optima XL-100 ultracentrifuge (Beckman Coulter) to remove cells and cell debris completely. The supernatants were then concentrated to ~1 mL (0.6 mg/mL) by using an Amicon Ultra centrifugal filter device (15 mL, 5K NMWL; Millipore). Protein in RPMI 1640 with 10% FCS was collected in the same way as the conditioned medium and used as a control. Total protein (120 μg) was fractionized with the ProteomeLab PF 2D Protein Fractionation System (Beckman Coulter). The separation was done using a PF2D HPRP column (Beckman Coulter) at 50°C with a flow rate of 0.75 mL/min. The column was equilibrated with solvent A [0.1% (v/v) trifluoroacetic acid in water] and eluted with solvent B [0.08% (v/v) trifluoroacetic acid in 100% (v/v) acetonitrile]. The gradient was 0% to 100% solvent B for 30 min. Eluent from column was automatically collected every 30 s into the 96-well plate with a fraction collector. Comparing the chromatogram profiles, fractions with peaks originating from FCS were excluded from further analysis. Fractions with specific peaks for cell culture supernatants were pooled into seven fractions, lyophilized, and resuspended in 100 μL of 20 mmol/L ammonium bicarbonate buffer (pH 8.0).

Two-dimensional liquid chromatography-MS/MS and data analysis. After trypsination of the fractions, two-dimensional liquid chromatography-MS/MS shotgun analysis was done by using an online nanoliquid chromatography system (Dina system, KYA Technologies) and a quadrupole time-of-flight mass spectrometer (Q-Tof Premier, Waters Micromass) as previously described (22). The identified proteins were obtained from MS/MS experiments by Mascot software (Matrix Science) using the Swiss-Prot human protein database containing 13,799 entries of human proteins (April 2006). The proteins were considered identified if they had resulting Mascot scores of >35 and at least two peptides with score >20. To determine the cellular localization of identified proteins, we used the information available from Swiss-Prot database.

cDNA microarray. Bladder cancer tissues for cDNA microarray analysis were obtained with informed consent from 55 patients who underwent surgery at our hospital. Tumor staging was assessed according to tumor-node-metastasis classifications (26 pTa, 11 pT1, 3 pT2, 13 pT3, and 2 pT4). Each bladder cancer sample was obtained by cold-cup biopsy at the time of transurethral surgery. As for the substitution of normal urothelium in the bladder, ureteral urothelium was obtained from 16 patients who had undergone nephrectomy for renal cell carcinoma. Ureteral urothelium was removed from the surgical specimen and the adjacent portion of the specimen was examined pathologically to confirm that neither urothelial dysplasia nor malignancy existed. Microarray experiments were done using a cDNA array containing ~30,000 50-mer oligonucleotides (MWG Biotech AG) fabricated by Pacific Edge Biotechnology Ltd. in New Zealand as described (23). In each hybridization, fluorescent cDNA targets were prepared from a tissue RNA sample and a reference RNA sample was derived from a pool of cell lines of different cancers. The

differences of gene expression profiles between T24 cells treated with anti-CXCL1 neutralizing antibodies or control IgG were examined by Human Genome U133 Plus 2.0 Array (Affymetrix, Inc.). cRNA preparation and hybridization to oligonucleotide arrays were according to Affymetrix protocol.

Reverse transcription-PCR. The primer sequences used for reverse transcription-PCR (RT-PCR) were as follows: CXCL1, 5′-CCAGACCCGCCTGCTG-3′ (forward) and 5′-CCTCCTCCCTTCTGGTCAGTT-3′ (reverse); CXCR2, 5′-ATTCTGGGCATCCTTCACAG-3′ (forward) and 5′-TGCACTTAGGCAGGAGGTCT-3′ (reverse); matrix metalloproteinase-13 (MMP-13), 5′-TCTGAACTGGGTCTTCCAAAA-3′ (forward) and 5′-GCATCTACTTTATCACCAATTCCT-3′(reverse); glyceraldehyde-3-phosphate dehydrogenase, 5′-GAAGGTGAAGGTCGGAGTC-3′ (forward) and 5′-GAAGATGGTGATGGGATTTC-3′(reverse). *Glyceraldehyde-3-phosphate dehydrogenase* was used as a housekeeping gene. Real-time quantitative PCR with SYBR Green was done using the GeneAmp 5700 Sequence Detection System (PE Applied Biosystems-Roche). The expression of MMP-13 was quantified relative to glyceraldehyde-3-phosphate dehydrogenase. The thermal profile consisted of 1 cycle at 95°C for 10 min followed by 40 cycles with 15 s at 95°C, 30 s at 60°C, 30 s at 72°C, and 10 s at 78°C. All measurements were done in duplicate.

Detection of CXCL1 proteins. Cells (3.5×10^5) were seeded in 60-mm dishes containing RPMI 1640 with 10% FCS. The medium was removed after 24 h, and the cells were then washed with PBS and further cultured in RPMI 1640 with 10% FCS. After 24 h, CXCL1 protein levels in cell-free culture supernatants were determined using the commercial Quantikine ELISA kit (R&D Systems) according to the manufacturer's instructions. Protein levels were corrected for the total protein in the cell lysate.

Immunohistochemical analysis. Tissues were fixed in 10% buffered formalin and embedded in paraffin. Paraffin blocks were cut at 5 μm thickness. Sections were deparaffinized and rehydrated. For CXCL1 staining, endogenous peroxidase activity was blocked with hydrogen peroxidase. The glass slides were washed in PBS (six times, 5 min each) and mounted with 1% rabbit normal serum in PBS for 30 min. Anti-human CXCL1 polyclonal antibody (1:150; Santa Cruz Biotechnology, Inc.) was used as the primary antibody. The sections were incubated overnight at 4°C, after which Histofine Simple Stain MAX PO (Nichirei Bioscience) was applied, and the subsequent antibody/enzyme conjugate was developed with diaminobenzidine. The sections were lightly counterstained with hematoxylin. MMP-13 staining was done by using an avidin-biotinylated peroxidase complex method (Vectastain Elite ABC kit, Vector Laboratories) as described by Bostrom et al. (24). Anti-human MMP-13 monoclonal antibody was from Daiichi Fine Chemical. A brown precipitate in the cytoplasm indicated a positive immunoreactivity in both proteins. Negative controls consisted of slides where the primary antibody had been omitted. Cases were evaluated as positive staining if >10% of the cytoplasm of the tumor cells was stained. All scoring was conducted in a blind fashion by a trained pathologist (Y.M.).

Knockdown of CXCL1 by RNA interference vector. Small interfering oligonucleotides specific for CXCL1 were designed on the Takara Bio Web site[7] and the oligonucleotide sequences used in the construction of the RNA interference (RNAi) vector were as follows: RNAi 1, 5′-GATCCGCACACTGTCCTATTATATTAGTGCTCCTGGTTGATATAATAGGACAGTGTGCTTTTTTAT-3′ and 5′-CGATAAAAAAGCACACTGTCCTATTATATCAACCAGGAGCACTAATATAATAGGACAGTGTGCG-3′; RNAi 2, 5′-GATCCGCAAATGGCCAATGAGATCATAGTGCTCCTGGTTGTGATCTCATTGGCCATTTGCTTTTTTAT-3′ and 5′-CGATAAAAAAGCAAATGGCCAATGAGATCACAACCAGGAGCACTATGATCTCATTGGCCATTTGCG-3′. The oligonucleotides were annealed and then ligated into *Bam*HI/*Cla*I sites of the pSINsi-hU6 vector (Takara Bio). A retroviral supernatant was obtained by transfection of G3T-hi cells using a Retrovirus Packaging Kit Ampho (Takara Bio). T24 cells were infected with the viral supernatant, and the cells were then selected with 750 μg/mL G418 for 2 to 3 wk. Stable CXCL1 knockdown clones were selected and confirmed by RT-PCR and ELISA.

Establishment of stable transformants of CXCL1. The full-length human CXCL1 cDNA was generated by RT-PCR using Pfu polymerase (Stratagene) from total RNA isolated from T24. The primers used for amplification were the following: 5′-CCAGACCCGCCTGCTG-3′ (forward) and 5′-CCTCCTCCCTTCTGGTCAGTT-3′ (reverse). The PCR product was ligated into *Xho*I/*Bam*HI sites of pcDNA3.1(-) vector (Invitrogen). RT112 cells were transfected with CXCL1 cDNA using Lipofectamine 2000 (Life Technologies, Inc.). Single clones of the stable transfectants were selected with 900 μg/mL G418. Each clone was checked for expression of CXCL1 by RT-PCR and ELISA.

Growth inhibition assay. RT112 and T24 cells (1×10^3 and 4×10^3, respectively) were seeded into 96-well plates in quintuplicate in RPMI 1640 with 10% FCS and allowed to adhere overnight. The cultures were then washed and refed with medium. Cells were incubated for 24 to 48 h. For treatment with neutralizing antibodies, monoclonal anti-CXCL1 or control antibody (mouse IgG; R&D Systems) was added to the medium. Proliferative activity was determined by the 3-(4,5-dimethylthiazol-2-yl)-2,5-diphenyltetrazolium bromide assay using a microtiter plate reader at 540 nm.

Measurement of urinary CXCL1 levels. Clean-catch urine specimens at clinic visits were collected throughout a period of several months from patients seen in our hospital. The control group consisted of outpatients attending with diseases of the urological tracts ($n = 31$, ages 48-84 y; benign prostatic hyperplasia in 14, prostate cancer in 9, lithiasis in 4, neurogenic bladder in 2, renal cancer in 1, and adrenal tumor in 1). Bladder cancer group consists of 67 patients (ages 47-90 y) before undergoing transurethral resection of bladder tumor for later histologically confirmed urothelial cancer (32 pTa, 23 pT1, and 12 pT2-4). There were no age differences between control group and bladder cancer group. These groups do not include the urine samples with >30 leukocytes/microscopic field. Collected samples were centrifuged for 10 min at 2,000 rpm at room temperature to remove debris, aliquoted, and stored -80°C. On the day of analysis, frozen urine samples were thawed quickly, and the urinary CXCL1 levels were measured using the Quantikine ELISA kit. Urine creatinine levels were measured spectrophotometrically using the alkaline picrate method.

Statistical analysis. The raw microarray data were analyzed using the nonparametric Mann-Whitney *U* test to compare the gene expression level between noninvasive pTa tumors and invasive pT1-4 tumors. The results of urinary CXCL1 levels were analyzed using the Mann-Whitney *U* test for two-group comparisons. The optimal sensitivity and specificity of the urinary CXCL1 levels for diagnosis of bladder cancer and for staging were determined by receiver operating characteristic (ROC) curve analysis using R statistical package. Univariable and multivariable logistic regression models were used to calculate odds ratios and 95% confidence intervals. Statistical analysis of the data was done using the StatView-J 5.0 program (Abacus Concepts, Inc.). A value of $P < 0.05$ was considered statistically significant.

Results

Evaluation of in vitro *invasiveness of bladder cancer cell lines and their proteome in cell culture supernatant.* We choose six different bladder cancer cell lines. Of them, three cell lines, DSH1, KU-7, and RT112 cells, are commonly used as models of superficial bladder cancer and UMUC-3, 5637, and T24 cells are generally used as models of invasive bladder cancer. Then, we examined their invasion ability *in vitro* by using a modified Boyden chamber assay. As shown in Fig. 1A, the number of cells infiltrated was higher in the latter group of cells; this result

[7] http://www.takara-bio.co.jp/

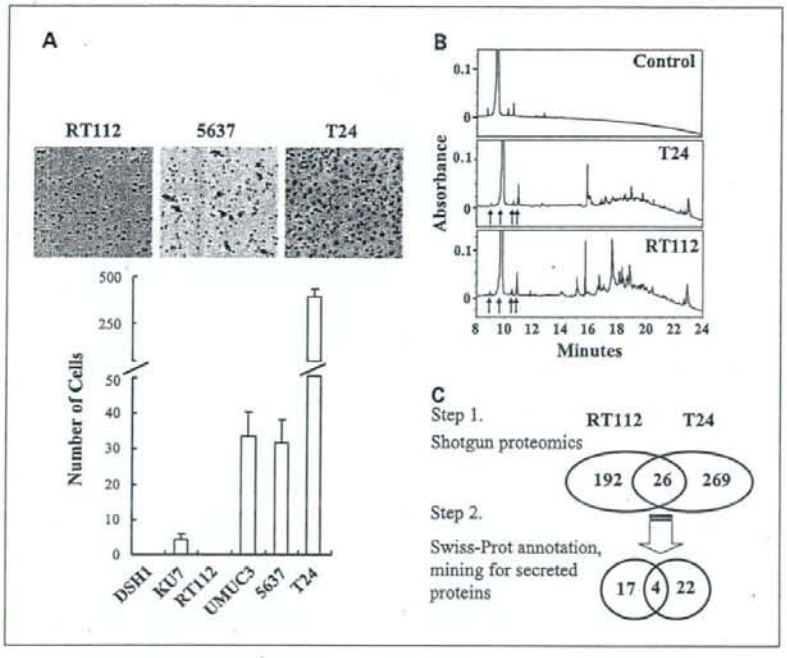

Fig. 1. *A*, invasion of bladder cancer cell lines in a modified Boyden chamber. Cells (5×10^4) were seeded into the upper compartment of the chamber in serum-free RPMI 1640 and incubated for 24 h at 37°C. RPMI 1640 with 10% FCS filled the lower compartment. Columns, mean of the number of cells in the five densest spots identified on the lower surface of the filter within a single ×200 field in each of three experiments; bars, SD. *B*, reverse-phase chromatograms of cell culture supernatants. Eluted proteins were detected by UV absorbance at 214 nm. In T24 and RT112 supernatant, peaks originating from FCS are indicated by arrows. The fractions from 11 to 23 min were collected for two-dimensional liquid chromatography-MS/MS analysis. *C*, schematic flow diagram depicting the steps for identifying proteins associated with invasion by human bladder cancer.

indicated that UMUC-3, 5637, and T24 are highly invasive, whereas DSH1, KU-7, and RT112 are poorly invasive tumor cells. DSH1 and RT112 showed almost no invasion ability and T24 cells exhibited the strongest invasive ability.

Because secreted proteins are thought to be suitable targets for the development of diagnostic markers and/or for identification of new drug targets (8, 9), we attempted to identify secreted proteins that were potentially involved or associated with the invasion of bladder cancer through the proteomic comparison of culture supernatants from highly invasive T24 and less invasive RT112 cells. As protein-rich FCS could easily mask proteins of interest in this analysis, we used serum-free medium as described previously (11, 12) and excluded contamination as far as possible by removing chromatogram fractions with peaks originating from FCS. As shown in Fig. 1B, fractions eluted from 11 to 23 min, which seemed to be produced from cultured cells, were pooled and analyzed by shotgun proteomics. A total of 477 proteins were identified in the culture supernatants of RT112 and T24 cells (218 and 295 proteins, respectively). Swiss-Prot database annotated the cellular localization of 330 proteins and 43 of them were predicted to be secreted proteins (Fig. 1C). Of these secreted proteins, 22 of them were detected only in highly invasive T24 cells (Supplementary Table S1).

Up-regulation of CXCL1 in invasive bladder tumors in vitro *and* in vivo. To further investigate the significance of these proteins in the invasion of bladder cancer, we compared the proteome data with mRNA expression profiles that consisted of 26 noninvasive pTa tumors and 29 invasive pT1-4 tumors *in vivo* (23). Among those 22 proteins specific for highly invasive T24 cells, there were corresponding probe sets for 14 of them on the custom-made chips. Of them, the expression of CXCL1 was significantly higher in invasive tumors than in noninvasive tumors *in vivo* (Fig. 2A). Additionally, the expression of this gene was more abundant in tumor tissues compared with that in normal uroepithelial cells. To confirm these results, the expression of this gene was examined in bladder cancer cell lines by using RT-PCR. It was revealed that all of the three highly invasive cell lines (UMUC-3, 5637, and T24) expressed CXCL1, whereas neither of them was detected in the less invasive DSH1, KU-7, and RT112 cell lines (Fig. 2B).

Because CXC chemokines are known to contribute to several tumor-related processes, such as tumor growth, angiogenesis/angiostasis, local invasion, and metastasis (25), we next examined the significance of CXCL1 in invasion of bladder cancer cell lines *in vitro*. First, we confirmed that all of the invasive cell lines secreted CXCL1 into the supernatants, whereas none of the less invasive cell lines secreted the detectable levels of this chemokine (Fig. 2C). These results indicate that higher secretion of CXCL1 is associated with the higher invasion ability of bladder cancer cells *in vitro*. It was also confirmed that *CXCR2*, the gene for the receptor of CXCL1, was expressed in all of bladder tumor cell lines irrespective of their invasion ability (Fig. 2B). Because CXCL1 was highly expressed at the mRNA level in invasive bladder tumors *in vivo*, we next examined if this chemokine is also up-regulated at the protein level. Representative results of immunohistochemical staining are shown in Fig. 2D. It was revealed that positive staining was observed in none of the normal uroepithelium samples and in 40% of pTa tumors. On the other hand, as many as 75% of pT1-4 tumors stained positive. These observations led us to hypothesize that the expression of CXCL1 was related to tumor invasion of bladder cancer *in vivo*.

Secreted CXCL1 is sufficient for increased invasion by bladder cancer cells. Next, we clarified whether CXCL1 regulated the invasive ability of bladder cancer cells *in vitro*. We first examined the effect of knockdown of CXCL1 in highly invasive T24 cells by using RNAi vectors. We have established two different polyclones in which the expression of CXCL1 is reduced by 30% compared with mock-transfected control cells (Fig. 3A). It was revealed that this inhibition of CXCL1 expression decreased the number of infiltrated cells in the invasion assay to 30% (Fig. 3B). Because the treatment of T24 cells with anti-CXCL1 neutralizing antibodies resulted in comparable reduction in the number of infiltrating cells, these results suggest that secreted CXCL1 regulates the invasive ability of bladder cancer cells via an autocrine loop (Fig. 3C). As CXCL1 has previously been shown to stimulate cell proliferation as an autocrine growth factor in several cancer cell lines (26, 27), we examined the effect of this chemokine on cell proliferation. As shown in Fig. 3D, the knockdown of CXCL1 or its neutralization with specific antibodies showed no direct effect on proliferation of T24 cancer cell lines. These results indicated that secreted CXCL1 in the supernatant promotes the invasion of T24 cells but has little effect on the proliferation of these cells.

To examine if the expression of CXCL1 is sufficient to promote the enhanced invasion of bladder cancer cell lines, less invasive RT112 cells were stably transfected with a plasmid that encoded CXCL1 and two independent monoclones were established. Both monoclones successfully secreted large amounts of CXCL1 and showed higher invasive ability compared with mock-transfected control cells (Fig. 3E). These results indicated that the expression of CXCL1 is sufficient to promote the enhanced invasion of bladder cancer cells *in vitro*. As observed for T24 cells, this effect was suppressed by treatment with anti-CXCL1 neutralizing antibodies and the forced expression of this chemokine had no effect on the proliferation of RT112 cells (data not shown).

CXCL1 regulated the expression of MMP-13 in bladder cancer cells in vitro *and the expression of CXCL1 was associated with that of MMP-13* in vivo. To clarify the mechanisms by which CXCL1 regulates the invasive ability of bladder cancer, we compared the mRNA expression profiles of highly invasive T24 cells treated with or without an anti-CXCL1 neutralizing antibody using the Affymetrix U133 Plus 2.0 Array. Among the 38,500 transcripts analyzed, we identified 62 RNAs whose abundance was decreased (<0.6-fold) by treatment with an anti-CXCL1 neutralizing antibody (Supplementary Table S2). It was revealed that a member of the MMP family, MMP-13, was down-regulated by the inhibition of CXCL1. To confirm this result, we examined the expression of MMP-13 in T24 and RT112 cells in which CXCL1 was engineered to be repressed or overexpressed, respectively. It was revealed that the expression of MMP-13 was regulated by the expression of CXCL1 in both cell lines (Fig. 4A). Because it has been reported that the expression of MMP-13 is associated with the invasion of bladder cancer *in vivo* (24), we next examined if the up-regulation of CXCL1 is associated with the higher expression of MMP-13 in bladder cancer cells *in vivo*. Positive staining of MMP-13 was observed in none of 11 tumors (6 with pTa, 4 with pT1, and 1 with pT3) with negative staining of CXCL1, whereas it was observed in 9 (1 with pT1, 7 with pT3, and 1 with pT4) of 19 (4 with pTa, 5 with pT1, 1 with pT2, 7 with pT3, and 2 with pT4) tumors with positive staining of that chemokine (Fig. 4B). It was revealed that statically significant correlation was observed between the expressions of both proteins ($P = 0.0064$, χ^2 test). These results suggest the possibility that MMP-13 is also regulated by CXCL1 *in vivo*.

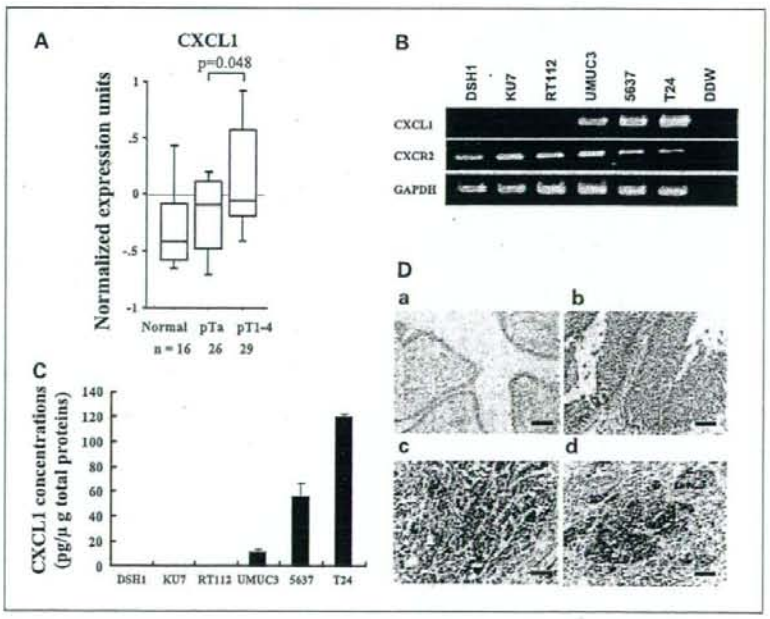

Fig. 2. *A*, cDNA microarray data for CXCL1. The normalized expression units of this gene were transformed into the log2 values. Bars of the box extend from the 25th to 75th percentile of the data and the line in the middle represents the median. The upper and lower bars represent the distance from the 10th to 90th percentile from the median. The Mann-Whitney *U* test was used to compare expression levels between the two groups. *B*, expression of CXCL1 and CXCR2 mRNA by bladder cancer cell lines with different levels of invasiveness. The PCR conditions are as follows: denaturation (95°C, 5 min), 32 cycles of denaturation (94°C, 1 min), annealing (58°C, 1 min), and extension (72°C, 1.5 min). GAPDH, glyceraldehyde-3-phosphate dehydrogenase. Values were corrected for the total protein in the cell lysate. *C*, expression of CXCL1 protein by bladder cancer cell lines. Protein levels in cell culture supernatants were analyzed by ELISA. Each cell line was plated in triplicate; experiments were repeated at least twice. Bars, SD. *D*, immunohistochemical staining for CXCL1 in surgical tissue specimens. A brown precipitate in the cytoplasm denotes positive signal. Representative samples of negative (*a*, normal uroepithelium; *b*, pTaG1) and positive (*c*, pT2G3; *d*, pT3G3) staining are shown. Bars, 100 μm.

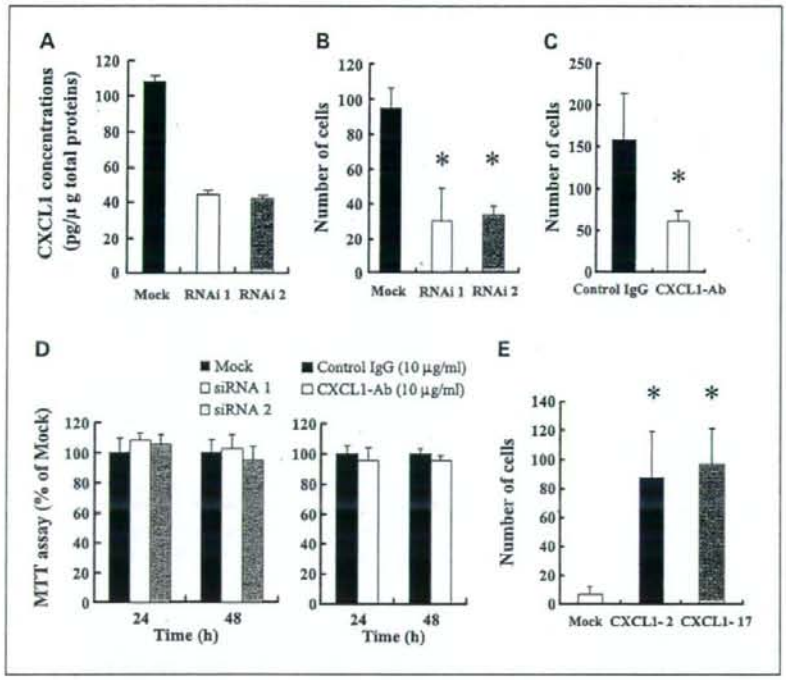

Fig. 3. *A*, knockdown of CXCL1 by RNAi vector in T24 cells was confirmed by ELISA. Values were corrected for the total protein in the cell lysate. Bars, SD. *B*, invasive potential of CXCL1 knockdown clones. After 8 h, the cells on the lower surface of the filter were counted. *, $P < 0.01$, compared with mock clones. *C*, effect of neutralizing antibody to CXCL1 on invasive ability. T24 cells were incubated in RPMI 1640 with 10% FCS containing 10 μg/mL anti-CXCL1 or control IgG for 48 h. Then, the cells were subsequently placed in the upper compartment of an invasion chamber in serum-free RPMI 1640 containing 10 μg/mL anti-CXCL1 or control IgG and incubated at 37°C under 5% CO_2. After 8 h, the cells on the lower surface of the filter were counted. *, $P < 0.05$, compared with control IgG. *D*, effect of CXCL1 knockdown and neutralizing antibody to CXCL1 on proliferation rate of T24 cells. The cell proliferation was determined by the 3-(4,5-dimethylthiazol-2-yl)-2,5-diphenyltetrazolium bromide (*MTT*) assay. No significant difference was detected. *E*, CXCL1 overexpression increased the invasiveness of RT112 cells. After 60 h of incubation, cells on the lower surface of the filter were counted. *, $P < 0.01$, compared with mock clones. Columns, each result of a modified Boyden chamber assay is expressed as the mean of the number of cells in the five densest spots identified on the lower surface of the filter within a single ×200 field in each of three experiments; bars, SD. A representative experiment is shown.

The level of CXCL1 in the urine reflects the existence of bladder cancer. Because immunohistochemical analysis showed that bladder tumors express CXCL1 *in vivo*, we determined if an increase of CXCL1 in the urine could indicate the existence of bladder cancer, especially that with invasive phenotype. The amount of CXCL1 in the urine was examined in 67 patients with histopathologically proven bladder cancer and 31 controls. Because it was shown that several chemokines are elevated in patients with febrile urinary tract infections (28), we eliminated urine samples contaminated with >30 leukocytes per microscopic field. The concentration of CXCL1 in the urine was examined by ELISA and corrected by the urinary creatinine level (Fig. 5A). The mean corrected CXCL1 level in the control group and in patients with noninvasive and invasive tumors was 7.8 ± 2.5, 17 ± 3.7, and 112 ± 25 pg/mg creatinine (mean ± SE), respectively. It was revealed that the corrected CXCL1 level from both noninvasive pTa tumors and invasive pT1-4 tumors was significantly higher than those in the controls ($P = 0.0076$ and $P < 0.0001$, respectively). More importantly, a significant difference was observed between noninvasive and invasive tumors ($P = 0.0028$). These results suggested that the corrected CXCL1 level in the urine would predict the existence of both noninvasive and invasive bladder tumors. So, we have done the ROC curve analysis to estimate the optimal cutoff point. Using 9.5 pg/mg creatinine as the cutoff value to predict the existence of noninvasive or invasive bladder cancer, measurement of the corrected urine CXCL1 level had a sensitivity of 70.1% and a specificity of 80.6% (area under the curve, 0.782; Fig. 5B). Furthermore, using 37.5 pg/mg creatinine as the cutoff value to predict particularly invasive bladder cancer, measurement of corrected CXCL1 had a sensitivity of 57.1% and a specificity of 90.6% (area under the curve, 0.713; Fig. 5C). Finally, we have done multivariate stepwise logistic regression analysis incorporating CXCL1 as a continuous variable, cytology, age, and sex to examine that the corrected CXCL1 level could be an independent factor for predicting the invasive bladder cancer. It was revealed that cytology (odds ratio, 21.82; 95% confidence interval, 3.981-113.780; $P = 0.003$) and CXCL1 (odds ratio, 1.023; 95% confidence interval, 1.001-1.044; $P = 0.038$) were independent factors for predicting the bladder cancer with invasive phenotype (Table 1).

Discussion

Tumor cells overexpress many secreted proteins; some of these can be detected in serum samples from patients with cancer and have been considered as potential new tumor markers (29). Well-known secreted proteins that are used as biomarkers include α-fetoprotein for liver cancer or non-seminomatous germ cell tumors, as well as prostate-specific antigen for prostate cancer (30). Our previous analysis of serum-free cell culture supernatants showed that proteins in the culture supernatant reflected those produced by tumor cells *in vivo* (11). This observation strongly suggests that systematic analysis of the proteins secreted by cultured cancer cells will contribute to the identification of potential diagnostic and prognostic tumor biomarkers.

We compared the protein profile between highly invasive (T24) and less invasive (RT112) bladder cancer cell lines.

Candidate proteins were further screened using the cellular localization information from the Swiss-Prot database. Consequently, CXCL1 was significantly higher in invasive tumors than in noninvasive tumors *in vivo* (Fig. 2A).

CXCL1 is a member of the CXC chemokine family (31). This family of molecules can be classified according to the presence or absence of three amino acid residues (Glu-Leu-Arg; ELR motif) that precede the first cysteine amino acid residue in the primary structure (32). The ELR$^+$ CXC chemokines (CXCL1, CXCL2, CXCL3, CXCL5, CXCL6, CXCL7, and CXCL8) are chemoattractants for neutrophils and are also potent angiogenic factors (33–35). In contrast, ELR$^-$ CXC chemokines (CXCL4, CXCL9, and CXCL10) are chemoattractants for mononuclear cells and are potent inhibitors of angiogenesis (35, 36). In a variety of human cancers, the ELR$^+$ CXC chemokines have been found to be associated with tumorigenesis, angiogenesis, and metastasis (25, 37). The biological functions of ELR$^+$ CXC chemokines are primarily mediated via CXCR2, a seven-transmembrane G protein–coupled receptor. CXCL1 protein was originally purified from the culture supernatant of Hs29T melanoma cells and is also known as melanoma growth stimulatory activity α or growth-related protein α (38, 39). Although the elevated expression of CXCL1 has been reported in a series of human tumors (40, 41), the role of this chemokine in bladder cancer is poorly understood. In this study, we showed that higher expression of CXCL1 was associated with the invasive phenotype of bladder cancer both *in vitro* and *in vivo* (Fig. 2). We also showed that the secreted CXCL1 was sufficient for the invasion of bladder tumors *in vitro* (Fig. 3). Because the CXCL1 receptor CXCR2 is expressed in all the bladder cancer cell lines (Fig. 2B) and in most of the tumor tissues examined irrespective of the invasion phenotype (microarray analysis; data not shown), it is probable that secreted CXCL1 is associated with the invasion of the bladder cancer via an autocrine loop involving its receptor.

CXCL1 did not induce bladder cancer cell proliferation, although it has been shown to promote cell proliferation in several types of tumors. Its interaction with CXCR2 is shown to induce extracellular signal-regulated kinase 1/2 phosphorylation, which then leads to induction of EGR1, and these are responsible for increased cell proliferation (37). Therefore, we examined the extracellular signal-regulated kinase 1/2 pathway in T24 and RT112 cells in which CXCL1 was engineered to be repressed or overexpressed, respectively. It was revealed that CXCL1 did not induce this pathway in bladder cancer cells (data not shown).

As for the mechanisms by which CXCL1 regulates the invasive ability of bladder cancer cells, we found for the first time that this chemokine induced MMP-13 *in vitro* (Fig. 4A). Although it is still uncertain if this is also true *in vivo*, a recent study showed that MMP-13 is highly expressed in invasive bladder tumor tissue (24), supporting our preliminary immunostaining results (Fig. 4B). As for other MMPs, Zhou et al. (42) reported that a glioma cell line overexpressing CXCL1 showed an increase in motility and invasiveness and that CXCL1-transfected cells showed increased expression of MMP-2. However, the expression of MMP-2 was not affected by the introduction of CXCL1 in RT112 cell lines (data not shown). CXCL1 may regulate the invasion of tumors through several types of MMPs. It has also been reported that this chemokine regulates the expression of several proteins, such as β_1 integrin, SPARC (42), vascular endothelial growth factor, and angiopoietin-2 (43). So, several factors including MMP-13 are likely to be involved in CXCL1-mediated regulation of bladder cancer invasion.

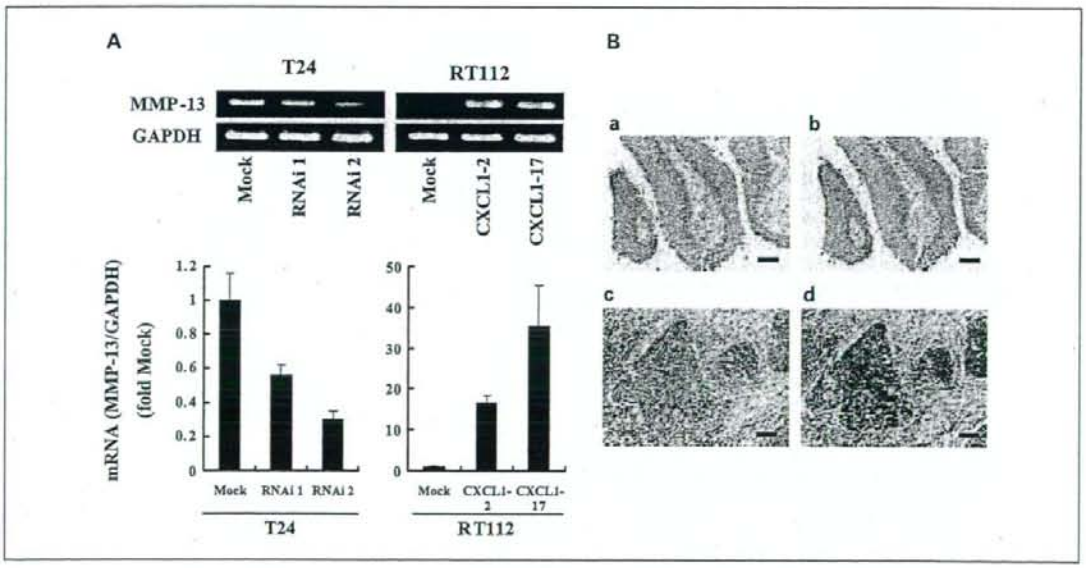

Fig. 4. *A*, expression of MMP-13 mRNA in T24 and RT112 cells in which CXCL1 was engineered to be repressed or overexpressed. RNAi knockdown of CXCL1 in T24 cells resulted in a decreased expression of MMP-13 and RT112 cells engineered to produce CXCL1 acquired the highly increased expression of MMP-13. Top, RT-PCR; bottom, real-time quantitative PCR. Bars, SD. *B*, immunohistochemical staining for CXCL1 and MMP-13 in bladder cancer tissues. Representative samples are shown. *a* and *c*, CXCL1; *b* and *d*, MMP-13. *a* and *b*, pT3G2 tumors showing diffuse cytoplasmic immunoreactivity; *c* and *d*, pTaG1 tumor without specific immunosignal. Bars, 100 μm.

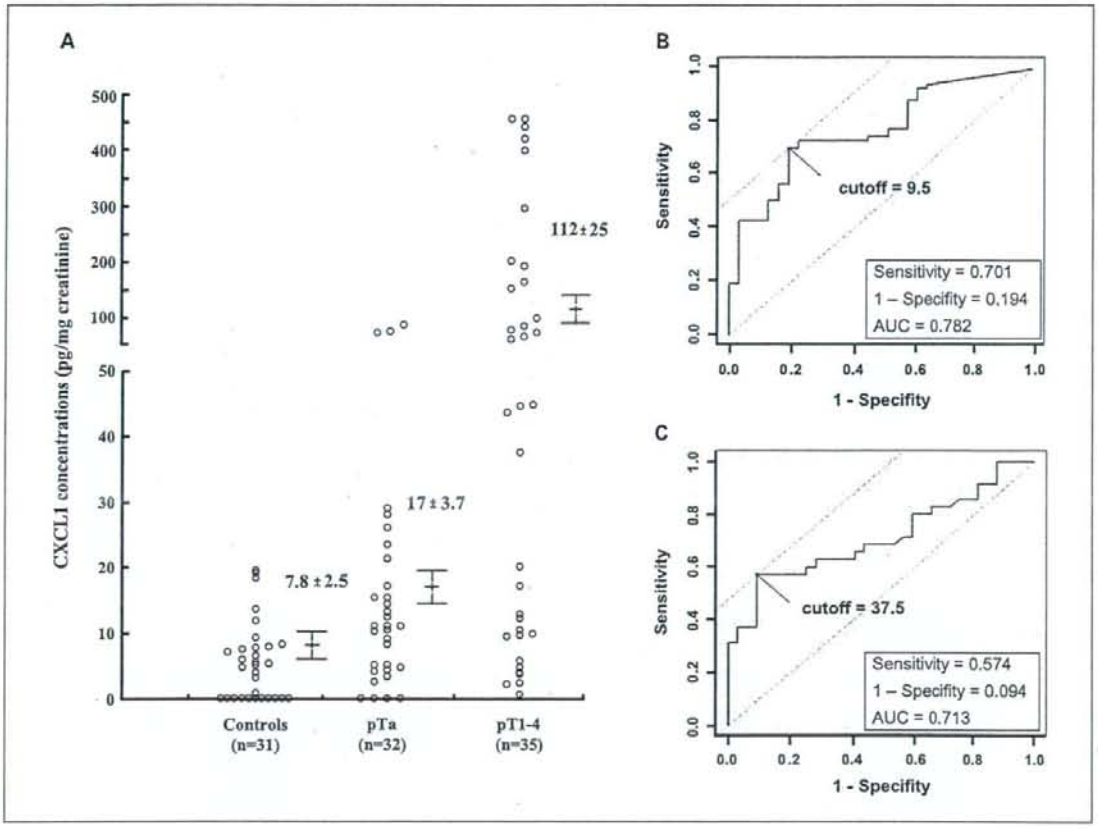

Fig. 5. *A*, CXCL1 levels in the urine of controls and patients with bladder cancer. Values were corrected by the urine creatinine concentration. Points, mean; bars, SE. *B*, ROC curve analysis of the urinary CXCL1 levels. The optimal cutoff of the urinary CXCL1 levels for distinguishing bladder tumor from control was determined as 9.5 using the ROC curve. *C*, ROC curve analysis of the urinary CXCL1 levels for distinguishing invasive from noninvasive bladder tumor. For all patients with bladder tumor, the optimal cutoff value of the urinary CXCL1 levels for distinguishing invasive from noninvasive bladder tumor was determined as 37.5 using ROC curve analysis.

Many studies have focused on the detection of specific bladder cancer–associated proteins in the urine of patients. Thus far, BTA, BTA stat, NMP22, and fibrinogen degradation products have been used as commercial diagnostic markers for bladder cancer in the urine (44). In addition, a lot of soluble urine marker is reported (45, 46). However, none of these markers is sensitive enough for routine clinical use (44). Recently, several investigators have proposed that high-throughput technologies, such as gene expression microarrays or proteomics, may be a new way to identify biomarkers for urothelial cancer in the urine (7, 47), and it is expected that this technology will be more widely used to identify novel cancer biomarkers in the future. In the present study, we showed for the first time that the level of CXCL1 was elevated in the urine from patients with bladder cancer (Fig. 5). These results indicate that an elevated CXCL1 in the urine could predict the existence of bladder cancer, especially in patients with invasive disease. Our results suggest that measurement of the level of CXCL1 in urine may be a useful biomarker for the early detection of invasive bladder cancer, and the inhibition of signals through CXCL1 might be a potent therapeutic target for preventing the progression of the bladder cancer. Additionally, CXCL8, one of ELR CXC chemokines that share 44% amino acid sequence identity with CXCL1 and are reported to be elevated in the urine of patients with transitional cell carcinoma (48). Further prospective and comparative studies in a different population are required for the precise evaluation of diagnostic values of CXC chemokines in bladder cancer.

Table 1. Multivariable stepwise logistic regression analyses of CXCL1, cytology, age, and sex for prediction of invasive stage (≥T1)

Variable	Odds ratio (95% confidence interval)	*P*
CXCL1*	1.023 (1.001-1.044)	0.038
Cytology (positive vs negative)	21.82 (3.981-113.7)	0.003

*Urinary CXCL1 levels were analyzed as continuous variables.